WIND TUNNEL TESTING FOR MEMBRANE STRUCTURES

Fernando, S., Georgiou, P.N. and Dutton, R.L.
VIPAC Engineers & Scientists Ltd.[1]

MSAA/LSAA Conf Proceedings

SUMMARY

Wind pressure distributions over pre-tensioned fabric roof structures are being investigated in an ongoing study using wind tunnel testing techniques. The results, obtained in terms of both local and pneumatically averaged "patch" pressures, enable the total differential wind loads under various typical configurations to be computed. This information will provide a foundation database to assist structural and fabric engineers in assessing the wind response of these structures. In this paper, some results from the study of conical shaped tent roofs are presented. Hypar shaped roofs are currently being investigated.

INTRODUCTION

With the development of material science and modern engineering construction techniques, fabric structures have become more and more common in our architectural environment. While wind loading is one of the most significant loads experienced by fabric roofs, relatively little documentation exists as to its characteristics. Most Wind Codes (e.g. AS 1170.2-1989) do not specify any guidelines to assist in their design, and engineers have had no alternative but to apply overly conservative wind loading estimates using data pertaining to structures considered to be similar in geometry.

The double curvature conical shape and hypar shape are the most common geometries used for pre-tensioned fabric structures. Hence these two classes of fabric structure were selected for examination in the current parametric study using wind tunnel model testing in order to define peak quasi-static wind loading on stiff roofs under different geometric conditions. Previous studies (Refs. 1-3) have shown that a rigid model of the undistorted fabric structure can be used to estimate the peak pressures experienced by its roof with reasonable accuracy. In the present study both local and pneumatically or "patch-averaged" (i.e. spatially and time-averaged) pressures were measured in order to provide loading information suitable for fabric and structural designers.

The geometries for the conical shaped tent structures chosen for study and the test variables such as under-blockage, apex opening covering, roof height, were made in consultation with members of the MSAA Technical Committee. The model tents represent typical geometries found in pavilions, open-air market enclosures, swimming pool covers etc.

---

[1] 275 Normanby Road, Port Melbourne, VICTORIA 3207
(Tel.) 03 - 647 9700, (FAX.) 03 - 646 4370

TEST GEOMETRIES

The Basic Tent Models

Rigid pressure models of two typical double curvature conical fabric roofs (referred to hereafter as the "tents") were constructed using fibreglass. A geometric scale of 1:50 was used to accommodate sufficient model detail considering the typical size of these structures. Both tent models are square in plan, approximately 30m x 30m full-scale. Both tents have an opening at the apex. The ring diameter, d, of this opening was kept constant, at d/w = 0.12 (where w = tent plan width).

The tents have significantly different curvatures - the "low" tent has a small radius of curvature, the "high" tent has a relatively high radius of curvature. The projected vertical height from edge level to apex of the low and high tents is 8m and 16m respectively.

Test Configurations

Four tests were carried out with each of the two tent models to investigate the effects of changes in the nature of blockage underneath the tent, covering of the apex and the relative height above ground of the tent.

Two support heights of 5m and 12m full-scale were used for both tents. These are referred to as "short" and "long" supports respectively. The apex covering was a hemispherical cap, full-scale diameter 3.9m, made of thickened fibreglass resin.

The simulated under-blockage consisted of a solid styrofoam block, with full-scale dimensions 24m x 24m x 4m, representing a non-porous structure located directly under the tent. The eight configurations tested are summarised in Table 1 below.

Pressure Tap Locations

The model tents were made of rigid fibreglass and instrumented with pressure taps to measure the wind pressures on both the outer and inner surfaces. In view of the axes of symmetry associated with the selected conical shape, one instrumented quadrant was able to fully define the pressure distribution over the whole roof. Two quadrants were instrumented in order to measure both discrete and patch-averaged pressures.

For the discrete pressure measurements, 47 pressure taps were mounted on the tent upper surface and another 47 on the lower surface at corresponding locations. For the patch-averaged measurements, each quadrant was sub-divided into four equal-area "patches". Each patch contained seven (7) manifolded taps which provided individual patch loads as well as total differential loads across the whole roof. The pressure tubing system used was tuned using constrictors to give an undistorted frequency response up to 50 Hz.

MSAA/LSAA Conf Proceedings

TABLE 1
Wind Tunnel Test Configurations
CONICAL ROOF TESTS

Test No.	Tent Type	Support Heights	Apex Cap Present	Under-Blockage
L - 1	Low	Short	No	No
L - 2	Low	Short	No	Yes
L - 3	Low	Short	Yes	No
L - 4	Low	Long	No	No
H - 1	High	Short	No	No
H - 2	High	Short	No	Yes
H - 3	High	Short	Yes	No
H - 4	High	Long	No	No

ATMOSPHERIC BOUNDARY LAYER SIMULATION

The models were tested at Vipac's Boundary Layer Wind Tunnel Facility in Port Melbourne, Victoria. The wind tunnel has a working section of 3m x 2m with a fetch length of 15m designed to achieve a fully developed boundary layer. The tunnel is powered by ten 10kW axial flow fans and is capable of producing mean wind speeds up to 22 m/s with correspondingly higher gust speeds.

After consultation with the MSAA Technical Committee, it was decided to use test wind conditions simulating Terrain Category 2 (AS 1170.2-1989), typical of open, flat terrain. For structures such as these, the worst wind loading is likely to occur in areas of high exposure, open areas. Rougher terrain has the potential for producing higher gust loading. However, this will be counteracted by lower mean loads arising from the additional shelter implied in the rougher terrain condition.

Measured longitudinal turbulence intensities, mean wind profiles and longitudinal spectra at apex height showed reasonable correlation with Terrain Category 2 representative values.

Modelling Similarity

Geometric similarity and kinematic similarity were maintained during the testing by keeping consistent length scales (at 1:50) for both the model tents and the boundary layer itself, and by proper scaling of the turbulence velocity characteristics of the wind tunnel flow. The highly turbulent nature of severe, design wind events means that thermal and/or

MSAA/LSAA Conf Proceedings

buoyancy effects can be ignored. The same cannot be said for Reynolds Number effects.

Reynolds Number Similarity

In establishing pressure distributions for body shapes with an aerodynamic profile, e.g. circular cylinders, the requirement that Reynolds Number equality be maintained is important for dynamic similitude. The Reynolds Number, basically a product of wind speed and typical building dimension, gives the ratio of the inertial forces to viscous forces. In the case of so-called "bluff" bodies (characterized by sharp edges) the resulting flow separation and pressure distribution remain essentially unchanged over a large range of Reynolds Number. In this case, the requirement of Reynolds Number similarity can be relaxed when determining gross reaction properties, resultant loads etc.

The model Reynolds Number used in this study is approximately 10^6, while the prototype or full-scale value is of the order of 10^8. For practical reasons, it is not possible to conduct wind tunnel model scale tests at comparable full-scale Reynolds Numbers - this would imply a tunnel test speed of over 1000 m/s! Reynolds Number effects were not investigated in detail in the present study. The tents under study however cannot be considered to be truly bluff bodies, and hence some variation in flow patterns will occur between full-scale and model scale. The following points should be noted:

(a) The peak pressure loads of interest occur near the leading and side edges of the tents and are largely unaffected by this phenomenon;

(b) Reynolds Number effects will be seen predominantly in changes to the pressure patterns after about mid-point along the tent cross-section in the direction of the flow. In this area, any variations in separation point will not provide a significant contribution to either the overall drag or uplift or downward load of the tent;

(c) The conservativeness of the method of calculating peak overall loads used in this study (see below) should compensate for any possible extra loading resulting from Reynolds Number mismatch.

TEST PROCEDURE

The eight model tent configurations shown in Table 1 were each tested for 16 wind azimuths, i.e. at 22.5° increments, with 0° taken as wind normal to a tent side face. A detailed description of the test equipment, pressure transducers, pneumatic tubing systems, scanivalve system, statistical analysis procedures etc. used to record the wind pressures on the tents is given in Vipac BT Report 10336 (1991).

The normal sign convention for surface pressures is **positive towards** the surface concerned and **negative away** from the surface.

MSAA/LSAA Conf Proceedings

The sign convention adopted in this study for the net differential pressures across a roof surface is **positive inwards** (i.e. **downwards**) and **negative outwards** (i.e. **upwards**).

Taking advantage of symmetry, the test results from all angles were compressed to give the variation of the peak pressures with the wind incident at 0° and 45°. The peak values for the 0° case were determined from the worst case peak values recorded at −22.5°, 0° and +22.5°. The worst case values recorded at 22.5°, 45° and 67.5° were used to develop the 45° peak pressures. Thus the two load cases, 0° and 45° included all maxima measured in the tests from all angles. As a consequence, a degree of conservativeness was introduced by taking worst case values in this manner.

For every upper and lower surface pressure tap pair, the peak positive net or differential pressure at that point of the roof was estimated by subtracting the lower surface peak negative pressure from the upper surface peak positive pressure. Similarly, the peak negative net pressure was estimated by subtracting the inner surface peak positive pressure from the upper surface peak negative pressure. Since the peak surface pressures on upper and lower tent surfaces are unlikely to occur at the same time, this addition of the individual peaks will also result in conservative estimates of the peak net pressure loads on the roof.

Pressure for all individual taps, tap pairs and also for the manifolded patch-averaging tap groups were recorded as dimensionless pressure coefficients. The pressures were normalised by the mean dynamic pressure at the height of the roof apex ring as defined below.

$$\textit{Mean Pressure:}\quad C_{\bar{p}} = \frac{\frac{1}{T}\int_0^T p(t)\,dt}{\frac{1}{2}\rho V_{ref}^2}$$

$$\textit{RMS Pressure:}\quad C_{\sigma_p} = \frac{\left[\frac{1}{T}\int_0^T (p(t)-\bar{p})^2\,dt\right]^{\frac{1}{2}}}{\frac{1}{2}\rho V_{ref}^2}$$

$$\textit{Maximum , Minimum Pressure:}\quad C_{\hat{p}} = \frac{p_{max}}{\frac{1}{2}\rho V_{ref}^2},\quad C_{\check{p}} = \frac{p_{min}}{\frac{1}{2}\rho V_{ref}^2}$$

MSAA/LSAA Conf Proceedings

where:

$p(t)$ = *instantaneous surface pressure*
T = *sampling period*
$\bar{p}$ = *time-averaged pressure*
p_{max} = *maximum pressure during period T*
p_{min} = *minimum pressure during period T*
V_{ref} = *reference mean wind speed at roof ring height*
ρ = *air density*

The choice of sampling period for individual pressure measurements was determined as follows. The sampling period, T, must be long enough to obtain statistically stable estimates of the mean, rms and peak values. Second, the measured peaks must be representative of the peaks that would be encountered during a full-scale interval of approximately one hour. Accordingly, the sampling period used in the current study was 120 seconds, which satisfies both of the above criteria.

RESULTS AND DISCUSSION

All test results have been included in Vipac BT Report 10336 (1991) soon to be released as a co-sponsored MSAA-Vipac Report. Only the peak pressures for selected configurations will be discussed in the current paper. In general the presence of a covering at the apex ring opening and the support height of the roof produced minor changes to the pressure distributions. The most significant parameters affecting the wind loads on the tents were the tent curvature and presence of under-blockage.

Peak Pressure Distributions

Figures 1 and 2 show the 0° and 45° differential pressure distributions for configurations L-1/L-2 and H-1/H-2 respectively. The following can be seen:

Peak Net Positive (PNP) Local Pressures:

- PNP pressure coefficients reached local maximum values close to 5.0;
- PNP pressures are greatest along the leading edge of all tents;
- For the low tent, under-blockage decreased the highest PNP pressures;
- For the high tent, under-blockage increased the highest PNP pressures.

Peak Net Negative (PNN) Local Pressures:

- PNN pressure coefficients reached local maximum values exceeding 4.0;
- PNN pressures are greatest just to the lee of the apex;
- For both tents, under-blockage increased the highest PNN pressures.

MSAA/LSAA Conf Proceedings

Peak Patch-Averaged Wind Loads

Figures 3 to 6 show both the 0° and 45° differential pressure coefficients for configurations L-1, L-2, H-1 and H-2 respectively. The following can be seen:

In general, the patch-average total differential loads are significantly lower than the local maxima discussed in the preceding section. This reflects the "smearing out" of the effects of intense but highly localised gust events which are responsible for the highest local pressures. Once again it is emphasized that the patch-averaged loads represent the actual area differential loads for each roof configuration and should be used when computing total or overall drag or uplift force for the tents. Integration of the discrete peak pressures discussed in the preceding section will be severely conservative.

Peak Net Positive (PNP) Pressure Patch-Average Coefficients:

- PNP coefficients range up to 2.0 and are significantly reduced in the presence of under-blockage;
- PNP loads are greatest towards the leading edge and away from the tent apex.

Peak Net Negative (PNN) Pressure Patch-Average Coefficients:

- PNN pressure coefficients can exceed 2.0;
- PNN pressures are greatest just to the lee of the apex and increase with the presence of under-blockage.

CONCLUSIONS

The comprehensive wind tunnel test programme carried out on the rigid models of conical square plan form fabric structures has shown that significant spatial variations in net wind pressure exist on the tent surface. The zoned (patch-average) pressure coefficients derived from these tests will assist in the design of more economical and functional wind-resisting structures, while the pressure local peak distributions should be used to identify "hot" spots in the design of fabric and fastening systems.

The presence of under-blockage and tent curvature induce significant variations in wind response for these structures. The relative roof support height also produces some local variations in peak total pressures on a roof. Covering the apex roof opening has negligible effect on roof loading.

MSAA/LSAA Conf Proceedings

REFERENCES

Jackson, P.S., "Flexible Tent Structures Under Dynamic Wind loading", University of Western Ontario, Engineering Science Research Report, BLWT-1-1983.

Ng, W.K., "External and Internal Pressures Induced Under the Turbulent Wind action on Arch-Roof Structures", M.E.Sc. Thesis, The University of Western Ontario, April 1983.

Johnson, G.L. and Surry,S., "Unsteady Wind Loads on Tents", University of Western Ontario, Engineering Science Research Report, BLWT-SS5-1985.

Surry, D. and Stathopoulos, T., "A Pneumatic Manifolding Technique for Spatially Averaged Unsteady Pressures", Proc. 6th Canadian Congress of Applied Mechanics, Vancouver, May 29-June 3 1977.

Holmes, J.D. and Osonphasop, C.,"Flow Behind Two-Dimensional Barriers on a Roughened Ground Plane, and Applications for Atmospheric Boundary Layer Modelling", 8th Australasian Fluid Mechanics Conference, University of Newcastle, Nov.28-Dec.2 1983.

"AS1170.2-1989 SAA Loading Code Part 2: Wind Loads", Standards Association of Australia, Standards House, North Sydney, NSW, 1989.

Lim, P. and Dean, B., "Influence of Geometry on Wind Pressure Coefficients on Conical Structures", MSAA Conference, Melbourne, 26-27 July 1990.

Fernando, S., Georgiou, P.N. and Dutton, R., "Wind Loading on Fabric Structures - Part 1: Conical Roofs", Vipac BT Report 10336, Vipac Engineers & Scientists Ltd, Port Melbourne, 1991.

MSAA/LSAA Conf Proceedings

MSAA/LSAA Conf Proceedings

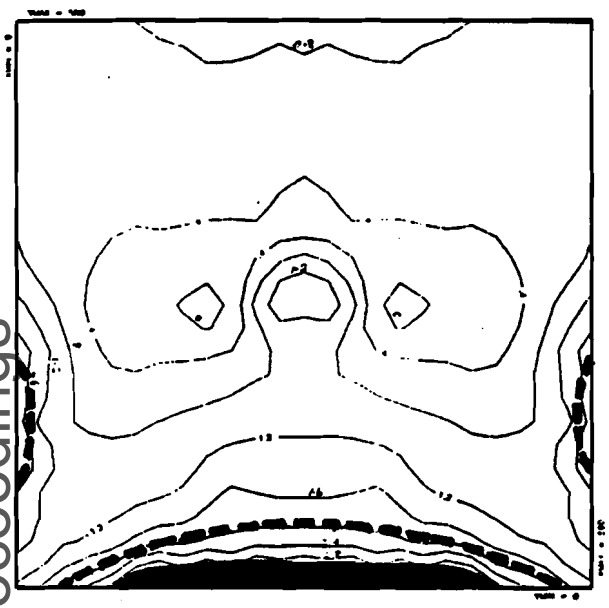

Tent L – 1 Peak POSITIVE

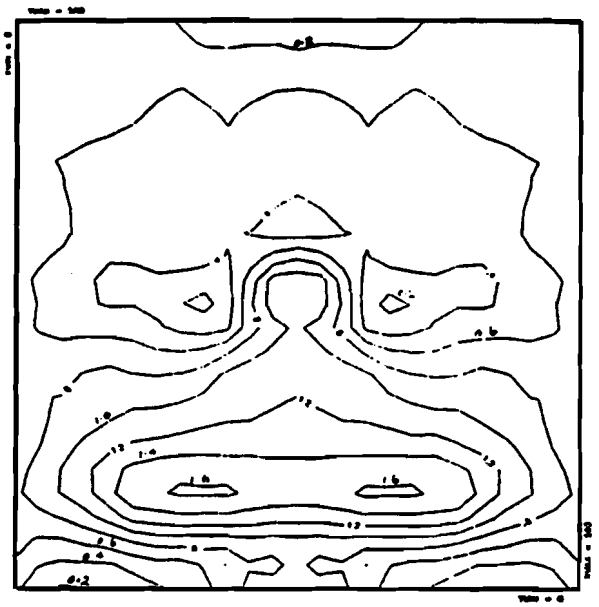

Tent L – 2 Peak POSITIVE

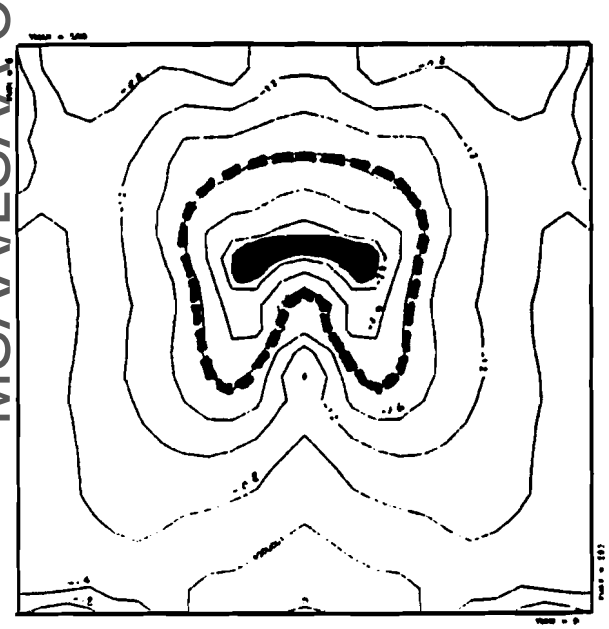

Tent L – 1 Peak NEGATIVE

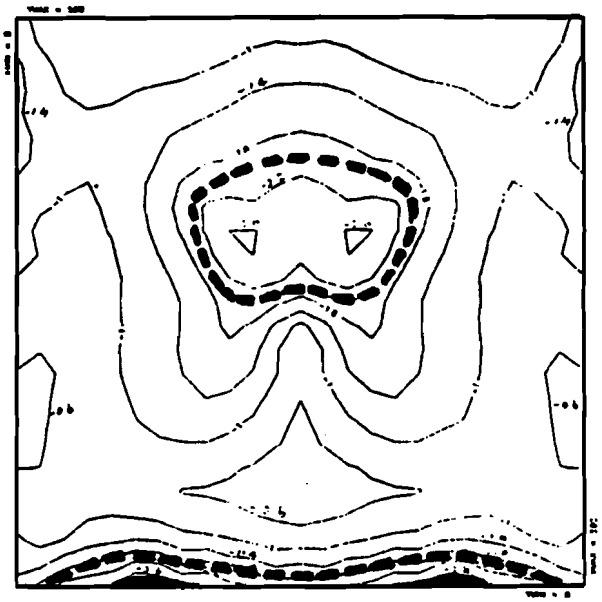

Tent L – 2 Peak NEGATIVE

Figure 1 Peak Local Pressure Distributions, Showing the Influence of Under-Blockage on the Low Tent Pressures

MSAA/LSAA Conf Proceedings

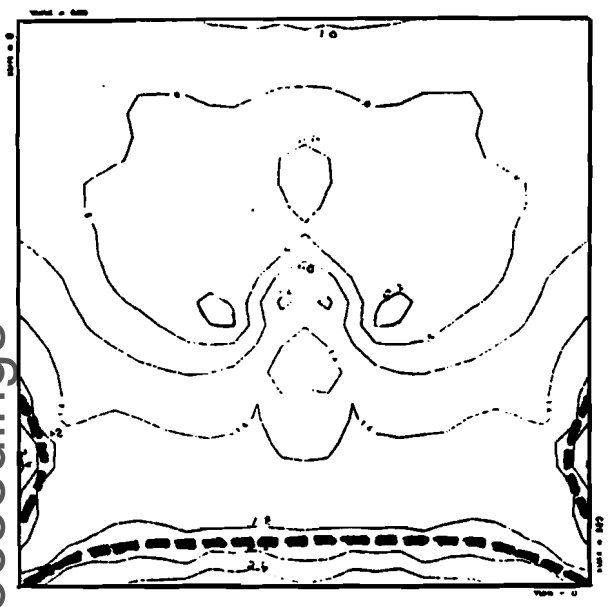

Tent H – 1 Peak POSITIVE

Tent H – 2 Peak POSITIVE

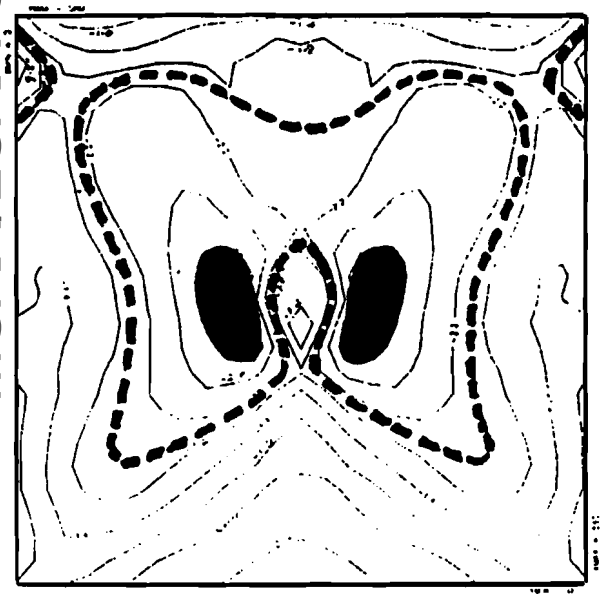

Tent H – 1 Peak NEGATIVE

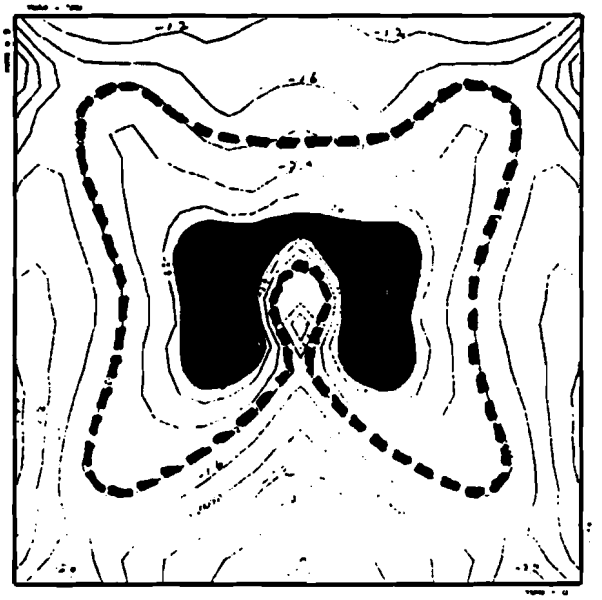

Tent H – 2 Peak NEGATIVE

Figure 2 Peak Local Pressure Distributions, Showing the Influence of Under-Blockage on the High Tent Pressures

MSAA/LSAA Conf Proceedings

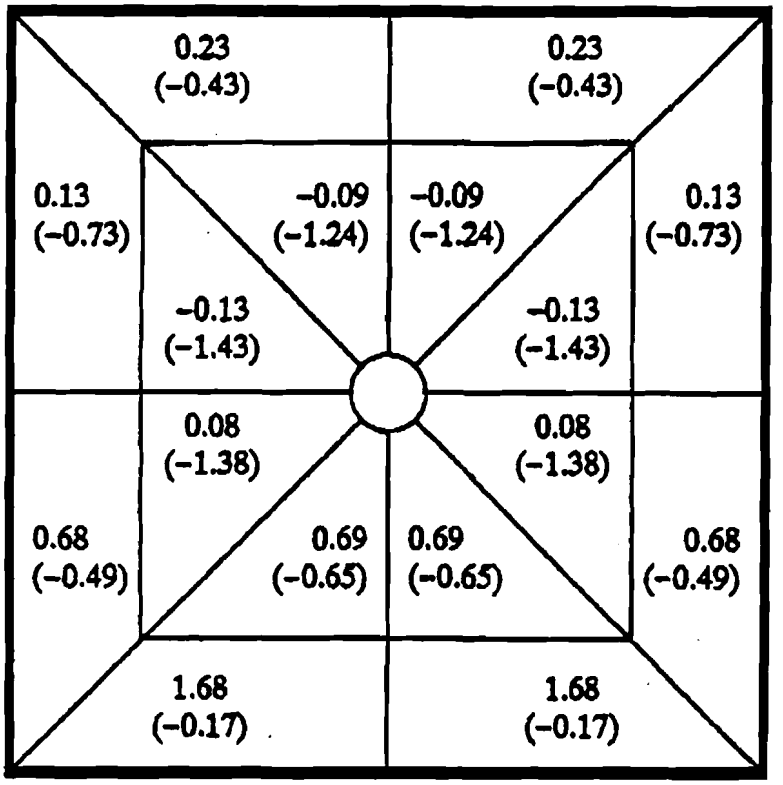

(a) 0° Wind Azimuth

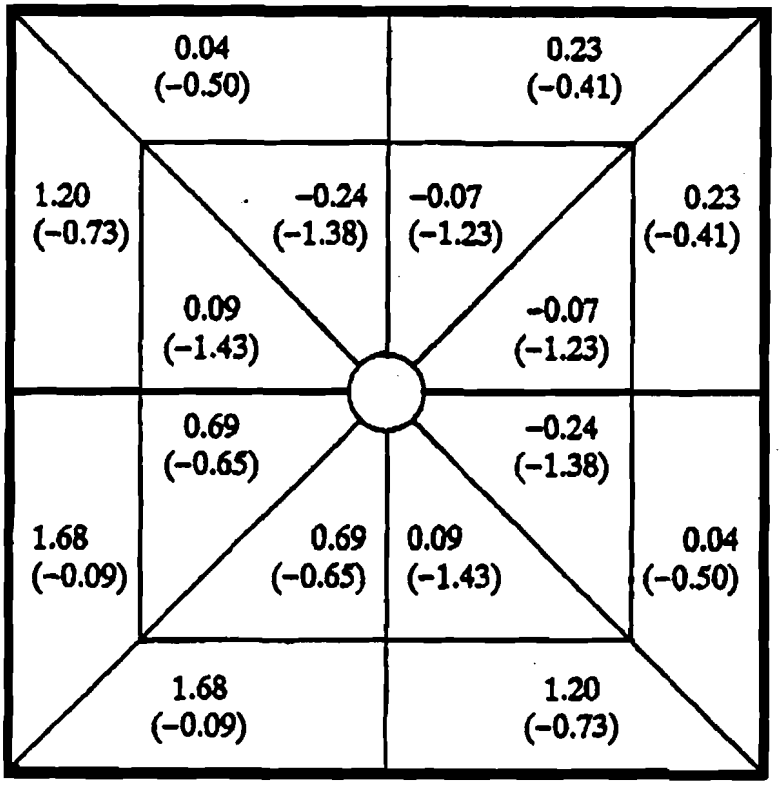

(b) 45° Wind Azimuth

Figure 3 Patch Averaged Peak Positive (Negative) Differential Pressures: Test L - 1

MSAA/LSAA Conf Proceedings

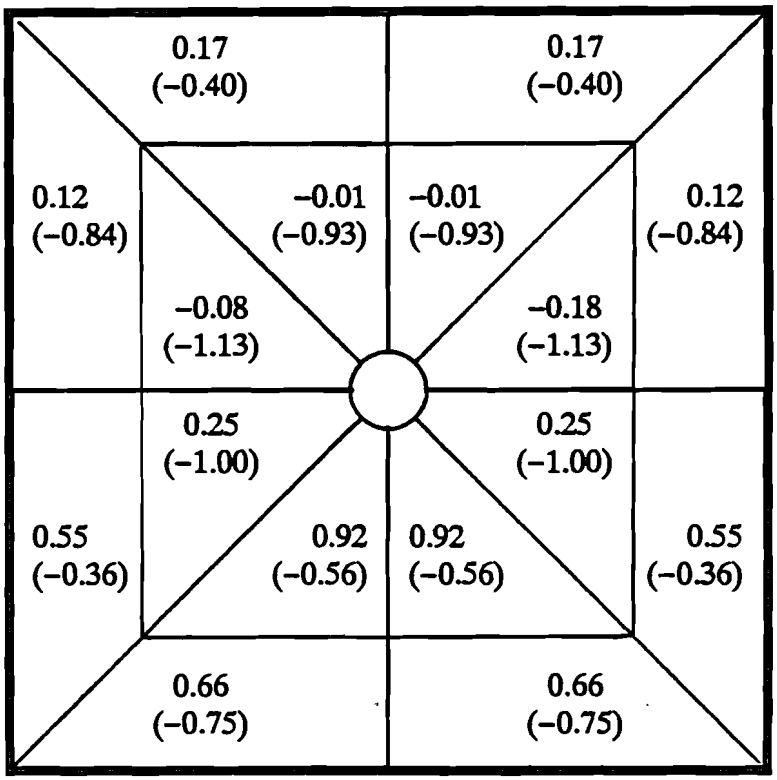

(a) 0° Wind Azimuth

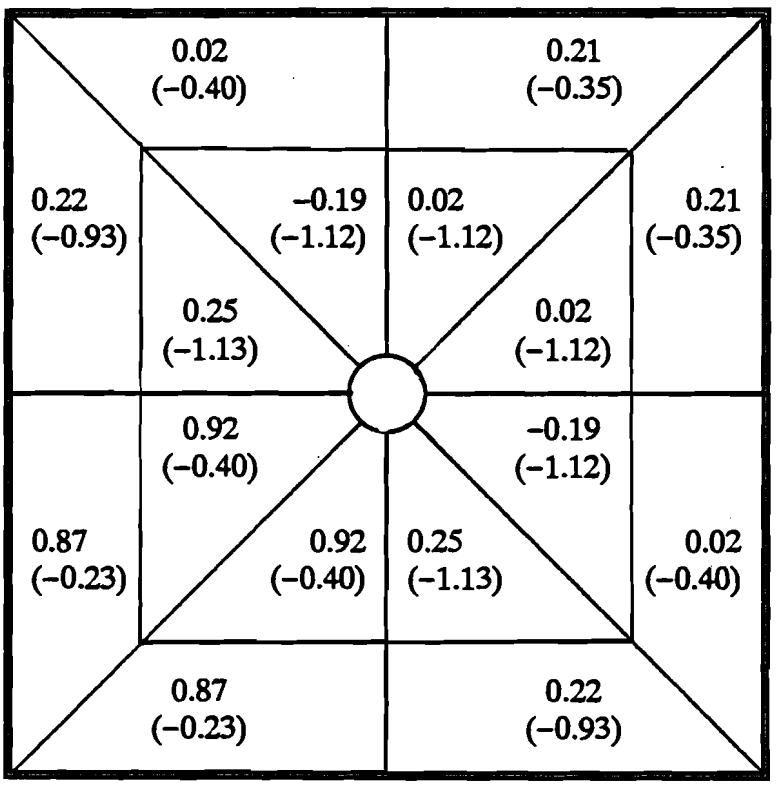

(b) 45° Wind Azimuth

Figure 4 Patch Averaged Peak Positive (Negative) Differential Pressures: Test L – 2

MSAA/LSAA Conf Proceedings

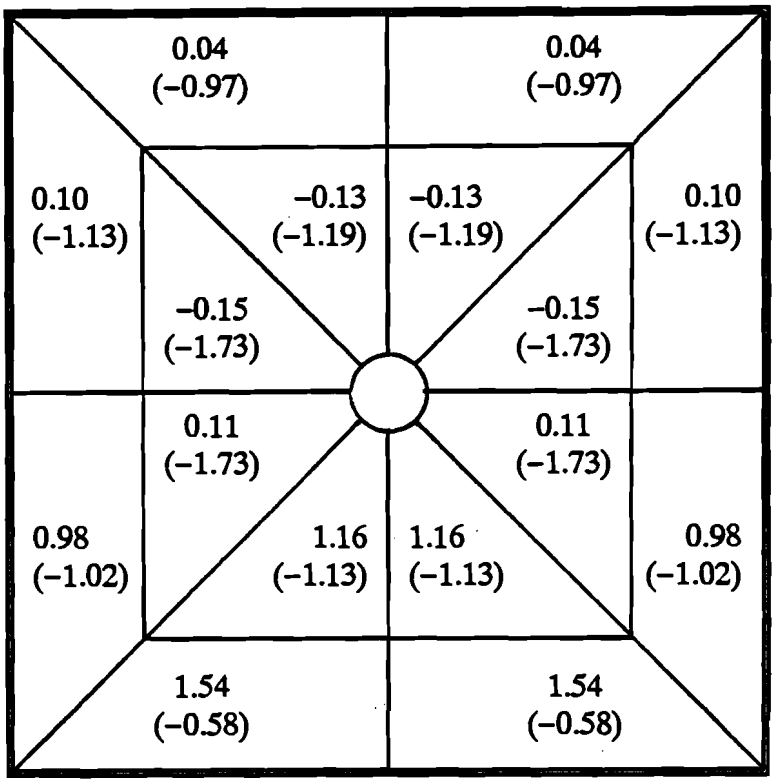

(a) 0° Wind Azimuth

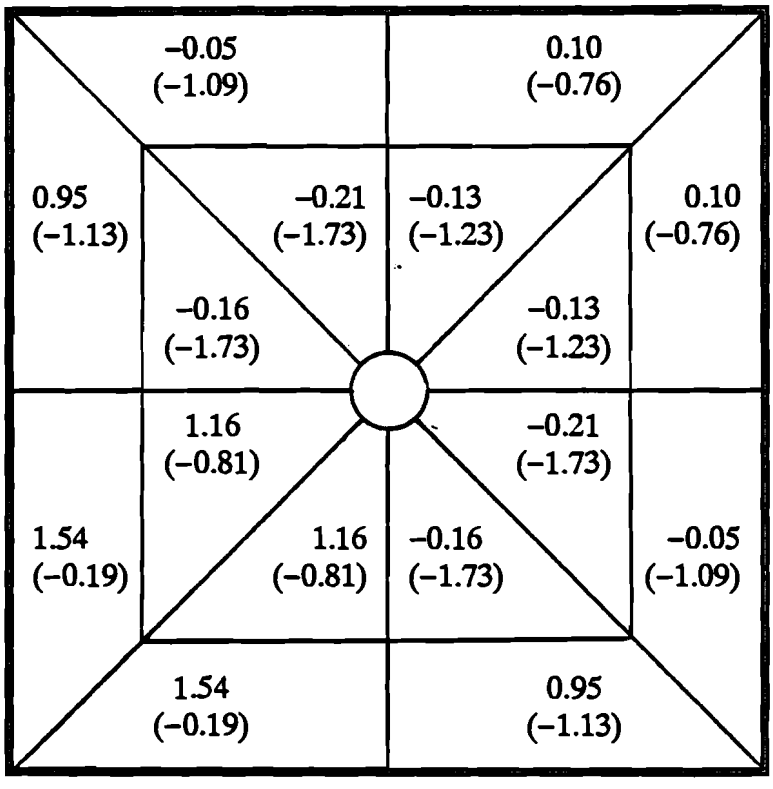

(b) 45° Wind Azimuth

Figure 5 Patch Averaged Peak Positive (Negative) Differential Pressures: Test H – 1

MSAA/LSAA Conf Proceedings

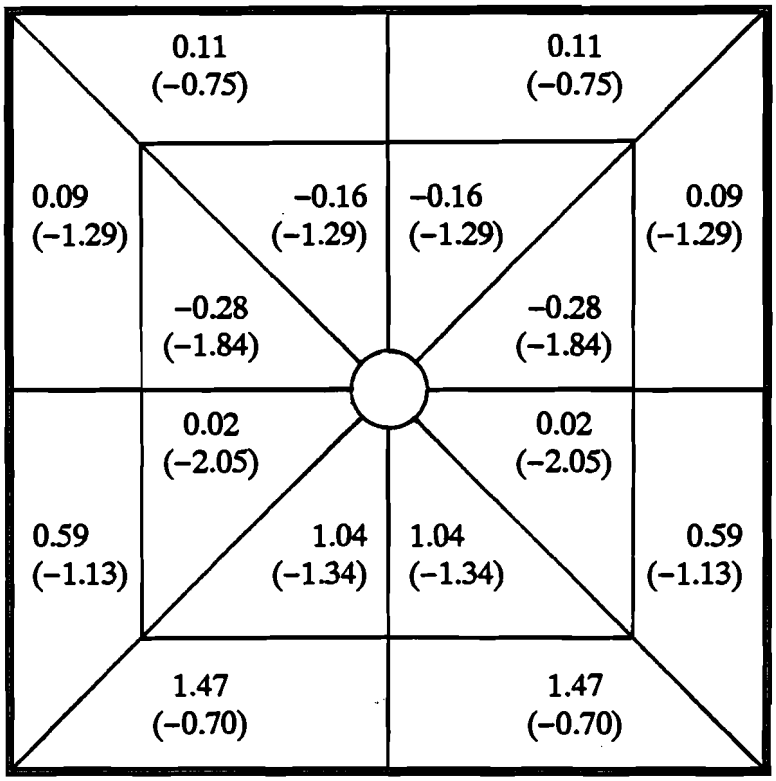

(a) 0° Wind Azimuth

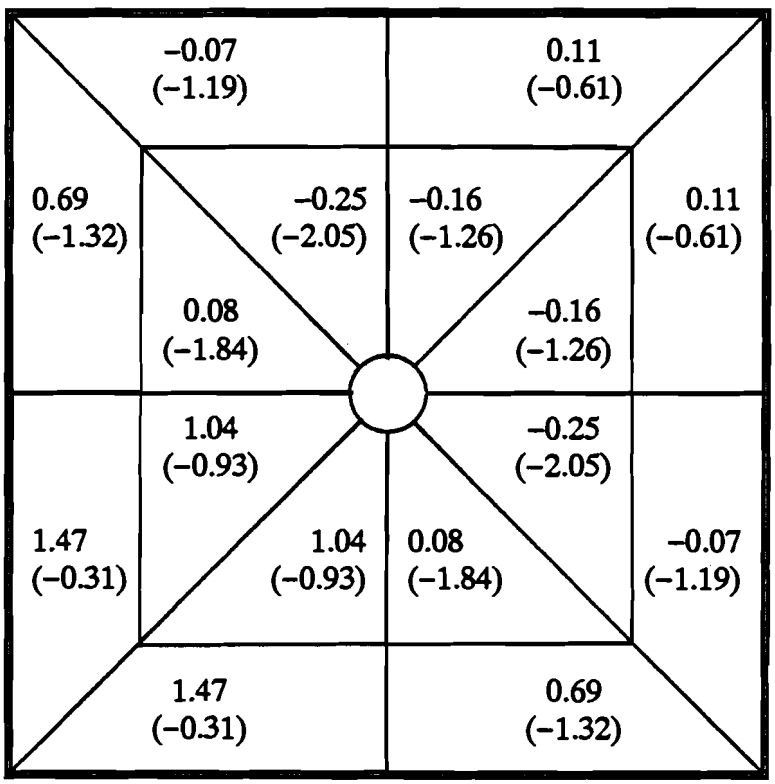

(b) 45° Wind Azimuth

Figure 6 Patch Averaged Peak Positive (Negative) Differential Pressures: Test H – 2